

# CITED1 Expression in Wilms' Tumor and Embryonic Kidney<sup>1</sup>

Harold N. Lovvorn III\*, Jenifer Westrup\*, Shaun Opperman\*, Scott Boyle†, Genbin Shi†, James Anderson‡, Elizabeth J. Perlman§, Alan O. Perantonι¶, Marcia Wills# and Mark de Caestecker†

\*The Department of Pediatric Surgery, Vanderbilt University School of Medicine, Nashville, TN, USA; †Division of Nephrology, and Cell and Developmental Biology, Vanderbilt University School of Medicine, Nashville, TN, USA; ‡University of Nebraska Medical Center, Omaha, NE, USA; §The Department of Pathology, Northwestern University, Chicago, IL, USA; ¶The Laboratory of Comparative Carcinogenesis, National Cancer Institute, Frederick, MD, USA; #Section of Pediatric Pathology, Vanderbilt University School of Medicine, Nashville, TN, USA

## Abstract

Wilms' tumors, or nephroblastomas, are thought to arise from abnormal postnatal retention and dysregulated differentiation of nephrogenic progenitor cells that originate as a condensed metanephric mesenchyme within embryonic kidneys. We have previously shown that the transcriptional regulator CITED1 (CBP/p300–interacting transactivators with glutamic acid [E]/aspartic acid [D]–rich C-terminal domain) is expressed exclusively in these nephrogenic progenitor cells and is downregulated as they differentiate to form nephronic epithelia. In the current study, we show that CITED1 expression persists in blastemal cell populations of both experimental rat nephroblastomas and human Wilms' tumors, and that primary human Wilms' tumors presenting with disseminated disease show the highest level of CITED1 expression. Unlike the predominantly cytoplasmic subcellular localization of CITED1 in the normal developing kidney, CITED1 is clearly detectable in the nuclear compartment of Wilms' tumor blastema. These findings indicate that CITED1 is a marker of primitive blastema in Wilms' tumors and suggest that persistent expression and/or altered subcellular localization of CITED1 in the condensed metanephric mesenchyme could play a role in Wilms' tumor initiation and pathogenesis.

*Neoplasia* (2007) 9, 589–600

**Keywords:** CITED1, Wilms' tumor, metanephric mesenchyme, nephroblastoma, nuclear localization.

adult nephrons. This process of mesenchymal-to-epithelial transition occurs reiteratively throughout nephrogenesis and is normally completed before birth in humans. Wilms' tumors typically comprise three cell types that are histologically reminiscent of those found in the developing kidney but that show no functionally organized tissue architecture. These cellular elements include undifferentiated blastema, primitive nephronic epithelia, and stroma [3,4]. A significant subset of kidneys from children who develop Wilms' tumor contains putative precursor lesions, known as nephrogenic rests, that also manifest histologic features of the condensed metanephric mesenchyme [5]. These observations have led to the hypothesis that Wilms' tumorigenesis is a result of abnormal postnatal retention and dysregulated differentiation of blastemal elements in the developing kidney.

Aside from histologic similarities, the strongest evidence supporting the embryonal origin of Wilms' tumor stems from early genetic studies that identified mutations in the *WT1* gene in 10% to 15% of patients who develop Wilms' tumors [6]. These findings provide evidence of a link between Wilms' tumorigenesis and defective embryonal development, as *WT1* is expressed in the developing kidney and plays a critical role in nephrogenesis [7,8]. In addition, a number of global gene array and expression studies have shown a significant overlap between Wilms' tumor and embryonic kidney gene expression profiles [9–11]. In Wilms' tumors, persistent expression of metanephric mesenchyme genes that are normally downregulated in the adult kidney includes *WT1* [12], *PAX2* [13], *SIX1*, *EYA1*, *SALL2*, and *HOXA11* [10]. However, there exists no mouse model that recapitulates Wilms' tumorigenesis

## Introduction

Wilms' tumor, or nephroblastoma, is the most common renal malignancy of childhood and is thought to arise from alterations in the coordinated differentiation of nephrogenic progenitor cells within the developing kidney. Normally, nephrogenesis occurs as a result of reciprocal tissue interactions between the ureteric bud (UB) epithelium, the condensed metanephric mesenchyme surrounding UB tips, and stromal mesenchyme [1,2]. These interactions coordinate the differentiation of the condensed metanephric mesenchyme into epithelial elements that give rise to functional

Abbreviations: CITED1, CBP/p300–interacting transactivators with glutamic acid [E]/aspartic acid [D]–rich C-terminal domain; UB, ureteric bud; COG, Children's Oncology Group; dp, days postcoitum

Address all correspondence to: Harold N. Lovvorn, III, MD, Suite 4150, 2200 Children's Way, Nashville, TN 37232-9780. E-mail: harold.lovvorn@vanderbilt.edu

<sup>1</sup>This work was funded, in part, by the Section of Surgical Sciences and the Ingram Cancer Center of the Vanderbilt University School of Medicine; by American Cancer Society Institutional Research Grant IRG-58-009-46; by the Intramural Research Program of the National Institutes of Health, National Cancer Institute, Center for Cancer Research (A.O.P.); and by R01DK61558 (M.d.C.).

Received 1 July 2004; Revised 30 June 2005

Copyright © 2007 Neoplasia Press, Inc. All rights reserved 1522-8002/07/\$25.00  
DOI 10.1593/neo.07358

*de novo*, precluding the use of mouse genetics to study whether persistent expression of these embryonic genes is necessary and/or sufficient to promote Wilms' tumorigenesis. The experimental model of Wilms' tumor that best mimics the histologic features of the human disease has been established in newborn rats after transplacental delivery of the alkylating agent *N*-ethylnitrosourea (NEU) [14–16]. These rats show a persistence of metanephric mesenchyme in the postnatal kidney that resembles nephrogenic rests in humans and, after a latency of 4 to 8 months, progresses to develop frank Wilms' tumors associated with typical triphasic cellular histology. Despite these observations, little progress has been made in understanding neoplastic mechanisms that promote the persistence of metanephric blastema and Wilms' tumorigenesis.

Recent studies from our laboratory have characterized the expression profile of the transcriptional regulator CITED1 (CBP/p300–interacting transactivators with glutamic acid [E]/aspartic acid [D]–rich C-terminal domain) during renal development [17–19]. CITED1 is expressed at high levels in the condensed metanephric mesenchyme surrounding UB tips, is downregulated temporally as these cells begin to differentiate into early epithelial structures, and is not expressed in differentiated elements of the adult kidney [19]. In the current study, we extend the embryonal characterization of Wilms' tumorigenesis by showing persistent expression of CITED1 within the blastemal compartment of both NEU-induced rat nephroblastomas and human Wilms' tumors. We show that CITED1 expression in rat and human nephroblastomas is associated with a shift in subcellular localization from the cytoplasm in the condensed metanephric mesenchyme to the nucleus in tumor blastema, and that the level of CITED1 expression in primary human Wilms' tumors correlates with tumor stage at presentation. These findings provide further evidence of the embryonal origin of Wilms' tumors and suggest that persistence and/or altered subcellular localization of CITED1 in the blastema could play a role in Wilms' tumor initiation and pathogenesis.

## Materials and Methods

### Rat Wilms' Tumor and Embryonic Kidney

To characterize the expression patterns of CITED1 in Wilms' tumor, we studied five experimental nephroblastomas that were induced transplacentally after exposing Noble fetal rats to *N*-nitroso-*N*-ethylurea, as described [16]. Briefly, at 17 days postcoitum (dpc), pregnant rats received an intraperitoneal injection of NEU (0.5 mmol/kg body weight). Dams were allowed to deliver naturally and to nurse their offspring, which were weaned and separated by sex at 4 weeks of age. Rats were killed when tumors became palpable or when animals became moribund. Tumor-bearing kidneys were processed and paraffin-embedded for tissue analysis. Normal fetal rat kidneys not exposed to NEU were harvested at 16.5 dpc and processed similarly. Animal studies were approved by the Institute for Animal Care and Use Committee of the National Cancer Institute.

### Human Wilms' Tumor and Embryonic Kidney

To characterize CITED1 expression patterns in human Wilms' tumor and to associate the CITED1 content of primary tumors with stage of disease, risk for disease relapse, and gender and age at presentation, we studied 20 favorable-histology Wilms' tumor (stages I–V) and 3 diffusely hyperplastic perilobar nephrogenic rest specimens (the typically blastemal and epithelial precursor lesion of Wilms' tumor; we did not study the more stromal Wilms' tumor precursor intralobar nephrogenic rest) provided by the Children's Oncology Group (COG). To minimize Wilms' tumor histology as a confounding variable on disease relapse, we restricted our studies to favorable-histology (no focal or diffuse anaplasia) specimens, given the highly lethal and more unpredictable biology of unfavorable-histology tumors. We received formalin-fixed paraffin-embedded histology slides and the corresponding “snap-frozen” whole-tissue specimens prepared from each of the 20 deidentified tumor patients. We were blinded to all patient and specimen data until the studies had been completed.

The COG chose 20 Wilms' tumor specimens to compare the CITED1 content of primary tumors among stage groups and to assess whether CITED1 tumor content was different in those patients who subsequently developed disease relapse. Diagnostic tumor samples were chosen to include patients at all stages (stages I–V) [20] and to oversample patients with disease relapse, as 10 of 20 patients whose primary tumors were studied subsequently relapsed (Table 1). This case–control–within-a-cohort study design permits the assessment of relationships between CITED1 content and patient characteristics, as well as the assessment of whether CITED1 content is predictive of disease relapse risk.

Discarded human fetal kidneys, one each for gestational ages 16 and 20 weeks, were procured from therapeutic abortuses (Advanced Bioscience Resources, Inc., Alameda, CA). Specimens were shipped overnight in sterile media on ice and fixed immediately on arrival in 10% buffered formalin.

The Institutional Review Board of the Vanderbilt University School of Medicine approved all studies involving human tumor and embryonic kidney specimens.

### Immunohistochemistry and In Situ Hybridization

To characterize the cellular distribution of CITED1 in rat and COG human specimens, we performed immunoperoxidase staining of formalin-fixed paraffin-embedded tissues (5- $\mu$ m sections). Tissues were incubated overnight at 4°C with affinity-purified rabbit anti-CITED1 antibody (1:50 dilution; Lab Vision Corp., Fremont, CA). Goat–anti-rabbit second-

**Table 1.** Distribution of Human Wilms' Tumor Samples, By Stage of Disease at Presentation and By the Presence or Absence of Disease Relapse.

	Stage I	Stage II	Stage III	Stage IV	Stage V	Total (N = 20)
Relapse-free	3	2	2	2	1	10
Relapse	2	2	2	3	1	10

ary antibody (1:250 dilution; Santa Cruz Biotechnology, Santa Cruz, CA) was applied to tissues at 37°C for 45 minutes, and tissues were visualized with a Vectastain ABC kit (Vector Laboratories, Burlingame, CA). Immunofluorescence was used to characterize CITED1 subcellular localization, and the protocol parallels that of immunoperoxidase staining by application of the secondary antibody. The TSA-Plus Fluorescein Amplification System (PerkinElmer Life Sciences, Boston, MA) was employed according to the manufacturer's protocol, and nuclei were stained with TO-PRO-3 Nuclear Stain (Molecular Probes, Eugene, OR). Tumor specimens were compared to embryonic kidneys for both rat and human tissues.

Subcellular localization of CITED1 was characterized as either predominantly cytoplasmic or mixed cytoplasmic and nuclear for rat and human specimens using confocal microscopy at  $\times 630$  original magnification (Carl Zeiss, Thornwood, NY; Cell Imaging Core, Vanderbilt University School of Medicine). The intensity of CITED1 detection was scored as absent, weak, intermediate, or strong by an independent observer (M.W.) who was blinded to all specimen data.

Using *in situ* hybridization, we also screened rat and human nephroblastomas for *CITED1* mRNA to determine whether increased CITED1 protein expression results directly from dysregulated gene transcription. *In situ* hybridization was performed as previously described [21], using 900-bp rat or human *CITED1* 35S-radiolabeled antisense or control sense probes on 10- $\mu$ m sections of 4% buffered paraformaldehyde-fixed paraffin-embedded rat or human tumor tissues, respectively. For images of tumor tissues, dark-field emulsion granules were converted to black and overlaid onto bright-field images to yield a dark signal where *CITED1* transcripts were detected.

#### Protein Extraction and Quantification

To quantify CITED1 expression in each of the 20 snap-frozen Wilms' tumor samples provided by the COG and to extract whole-tissue protein, specimens were homogenized in lysis buffer containing protease inhibitors and sonicated to disrupt cellular integrity, as described [22]. The protein content of tissue lysates was determined after clarification by Bradford assay, and an equivalent protein loading was confirmed by Western blot analysis for  $\beta$ -actin (anti- $\beta$ -actin mouse monoclonal antibody; Sigma-Aldrich, St. Louis, MO). To optimize CITED1 detection between samples, an equal quantity of protein from each specimen was immunoprecipitated using an affinity-purified rabbit anti-CITED1 antibody raised against residues 178 to 193 of the CITED1 C-terminus, as described [23]. Immunoprecipitates were then separated by sodium dodecyl sulfate–polyacrylamide gel electrophoresis, transferred to PVDF membranes, and probed with the mouse MoAb anti-CITED1 antibody 2h6 [17,22]. To estimate protein concentrations for each sample, CITED1 band intensities were quantified by densitometry (EpiChem<sup>3</sup>; UVP Bioimaging System, Upland CA), and results were normalized as the ratio of CITED1 to  $\beta$ -actin band densities for each preparation.

#### Data Analysis

As the CITED1 content of primary human Wilms' tumors appeared to be normally distributed, we used linear regression methods to predict the mean CITED1 content as a function of stage and "relapse" status. After adjusting for the differences in CITED1 levels seen by stage of disease (stages I–III only), we further queried whether CITED1 content of primary tumors differed according to gender and age at presentation. All statistical analyses were performed using SAS (Cary, NC). Significant differences were determined for  $P < .05$ . All data points were represented using box plots.

## Results

#### *CITED1* Expression in Rat Embryonic Kidneys and Experimental Nephroblastomas

To characterize CITED1 expression patterns in embryonic and malignant blastemas, we initially analyzed rat embryonic kidneys and NEU-induced nephroblastomas. As expected in rat embryonic kidneys, CITED1 expression is localized strictly to the condensed metanephric mesenchyme surrounding UB tips, and its expression is lost as the condensed metanephric mesenchyme differentiates into the earliest epithelial structure, the renal vesicle (Figure 1A) [17]. The specificity of the antibody has been confirmed with negative immunostaining in *Cited1*-null mutant mice that develop normal aggregates of the condensed metanephric mesenchyme and structural nephrons [19]. Using this same antibody, we detected widespread CITED1 expression in disorganized blastemal compartments of rat nephroblastomas and no expression in primitive tubular, glomerular, or stromal elements of these tumors (Figure 1B). In certain tumor regions showing blastemal-to-epithelial transition, CITED1 expression is strongest in peripheral blastema, with absent or weak expression in the central more differentiated tumor cells (Figure 1C, arrows).

We next performed immunofluorescence analysis to discriminate carefully the subcellular localization of CITED1 within these two tissue types. As previously reported in mouse embryonic kidneys [18,19], CITED1 is localized almost entirely to the cytoplasmic compartment of the condensed metanephric mesenchyme within rat embryonic kidneys (Figure 2, A and B). In contrast, CITED1 is detectable in both the nuclear compartment and the cytoplasmic compartment of blastemal cells in rat nephroblastomas (Figure 2, C and D). In a count of 137 CITED1-positive metanephric mesenchyme cells within rat embryonic kidneys ( $n = 2$ ), only 15 (10.9%) cells showed visible nuclear expression of CITED1, which was weak in intensity. In contrast, 359 of 434 (82.7%) CITED1-positive blastemal cells within rat Wilms' tumors ( $n = 2$ ) showed a strong nuclear expression of CITED1 (Figure 2E).

#### *CITED1* Expression in Human Embryonic Kidneys, Wilms' Tumors, and Perilobar Nephrogenic Rests

Having established the expression patterns of CITED1 in rat embryonic kidneys and nephroblastomas, we proceeded

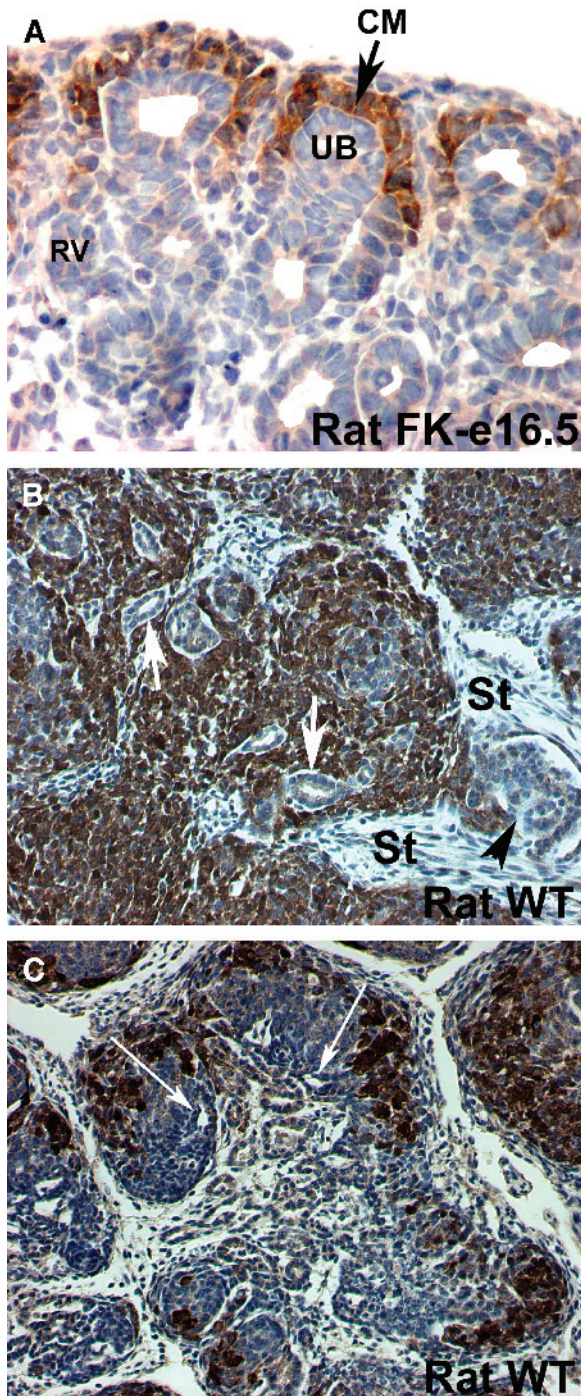


**Figure 1.** CITED1 immunoperoxidase staining (brown) of rat fetal kidney (A) and NEU-induced nephroblastoma (B and C). (A) CITED1 expression in rat fetal kidney (FK) 16.5 dpc is restricted to the condensed metanephric mesenchyme (CM) immediately adjacent to and surrounding UB tubular structures (original magnification,  $\times 400$ ). Note the absence of CITED1 expression in the early renal vesicle (RV) epithelia of mesenchymal origin. (B) CITED1 expression in rat nephroblastoma (WT) is intense in blastemal elements (brown) and absent in primitive epithelia (white arrows, tubules; black arrowhead, glomerulus) and stroma (St) (original magnification,  $\times 400$ ). (C) The region of blastemal-to-epithelial transition shows downregulation of CITED1 expression in a gradient from positive peripheral blastema to negative central epithelia (arrows) (original magnification,  $\times 200$ ).

to evaluate its expression in human tissue samples. CITED1 expression is restricted to the condensed metanephric mesenchyme of human embryonic kidneys of 16 and 20 weeks' gestation (Figure 3, A and B), and it is highly expressed in disorganized blastemal compartments of human Wilms' tumor samples (Figure 3, C and D). Unlike normal human embryonic kidneys, CITED1 is detectable in primitive epithelial structures in some (Figure 4), but not all (Figure 3D), Wilms' tumor samples. Rare primitive tubular structures in the form of rosettes show an intermediate intensity of CITED1 expression (Figure 4A), yet more mature-appearing epithelial structures show a weak and cytoplasmic expression of CITED1 (Figure 4B). As in the rat nephroblastoma model (Figure 1C), certain human tumor regions show a CITED1 expression gradient from greater intensity in peripheral blastemal cells (also lacking organized architecture) to weak cytoplasmic expression in the more organized tubular portion (Figures 3D and 4C). Semiquantitative evaluation of the 20 COG human WT samples showed that 13 of 15 mixed tumor types displayed weak or intermediate staining of CITED1 in primitive epithelial structures (Table 2).

Consistent with data in rat embryonic kidneys and experimental nephroblastomas, confocal imaging of CITED1 expression confirmed dominant cytoplasmic localization in the condensed metanephric mesenchyme of the human embryonic kidney, whereas CITED1 was clearly detected in the nuclear and cytoplasmic compartments of blastemal cells within human WT samples (Figure 5). Immunofluorescent staining of human fetal kidneys shows that CITED1 expression is restricted to the condensed metanephric mesenchyme and is localized predominantly to the cytoplasm of this progenitor cell population (Figure 5A). CITED1 expression is intense in malignant blastema and, in contrast to the embryonic state, is robustly detected in the nuclei of this transformed cell population (Figure 5, B and C). Aggregation and differentiation of blastema show downregulation of CITED1 expression relative to disorganized blastema (Figure 5B).

Of the 20 COG Wilms' tumor tissue sections, areas of blastemal and epithelial elements were present in 17 and 13 samples, respectively—sufficient to perform a detailed evaluation of CITED1 immunostaining in these cellular subtypes (Table 2). Disorganized blastemal regions in each tumor (100%) showed nuclear CITED1 localization of variable intensity. In contrast, primitive epithelia in 3 of 13 (23%) tumors showed CITED1 nuclear expression, yet more organized epithelia in the remaining 10 tumors showed variable intensity of CITED1 expression restricted to the cytoplasm. Seven of 17 (41%) tumors having sufficient blastema showed strong CITED1 nuclear expression in disorganized blastemal regions, whereas only 1 of 13 (8%) tumors having sufficient epithelia showed strong CITED1 nuclear expression within epithelial elements. Interestingly, the COG had classified this latter tumor as "epithelial undifferentiated."

Immunostaining of perilobar nephrogenic rests, which are considered neoplastic precursors of Wilms' tumor, showed a similar pattern of mixed nuclear and cytoplasmic staining in the blastema, with weak cytoplasmic staining in associated epithelial, but not stromal, structures (Figure 6).

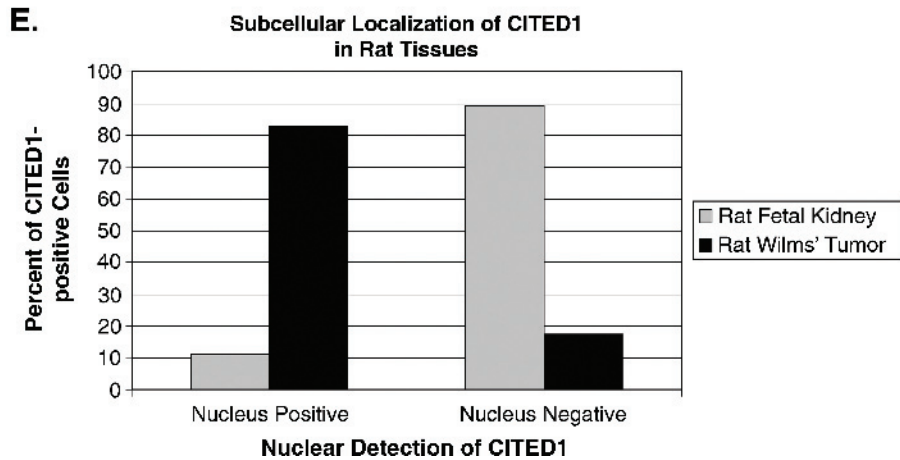
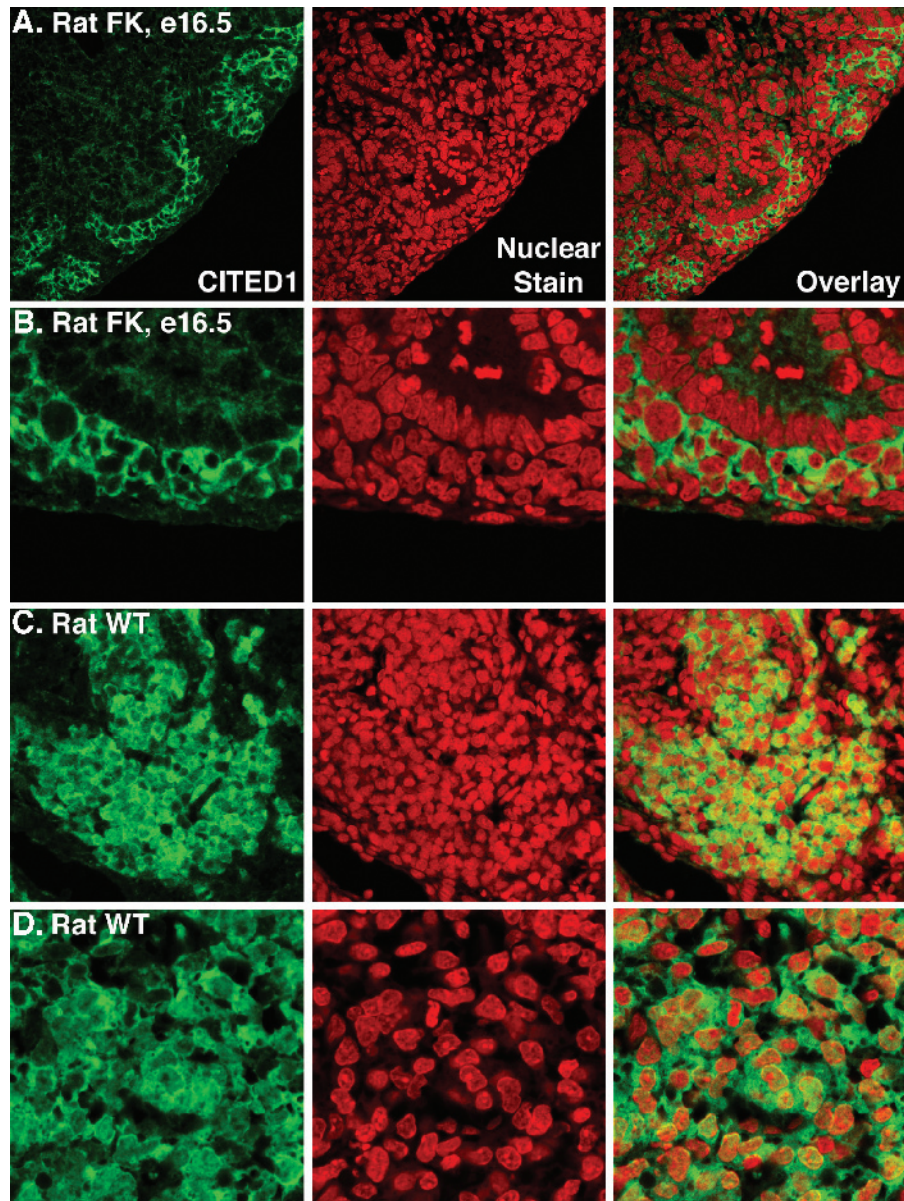


**Figure 2.** CITED1 immunofluorescent staining (green) of rat fetal kidney (rows A and B) and NEU-induced nephroblastoma (rows C and D). TO-PRO3 nuclear stain appears red. (A) Original magnification,  $\times 200$ ; (B) original magnification,  $\times 400$ . (A and B) CITED1 is detected predominantly in the cytoplasm of the condensed metanephric mesenchyme in rat fetal kidneys (FK) 16.5 dpc, whereas in rat Wilms' tumor (WT), CITED1 is richly detected in the nuclear and cytoplasmic compartments. (C) Original magnification,  $\times 400$ ; (D) original magnification,  $\times 630$ . (E) In cells expressing CITED1, rat WT showed markedly greater and more visible nuclear accumulation than the condensed metanephric mesenchyme.

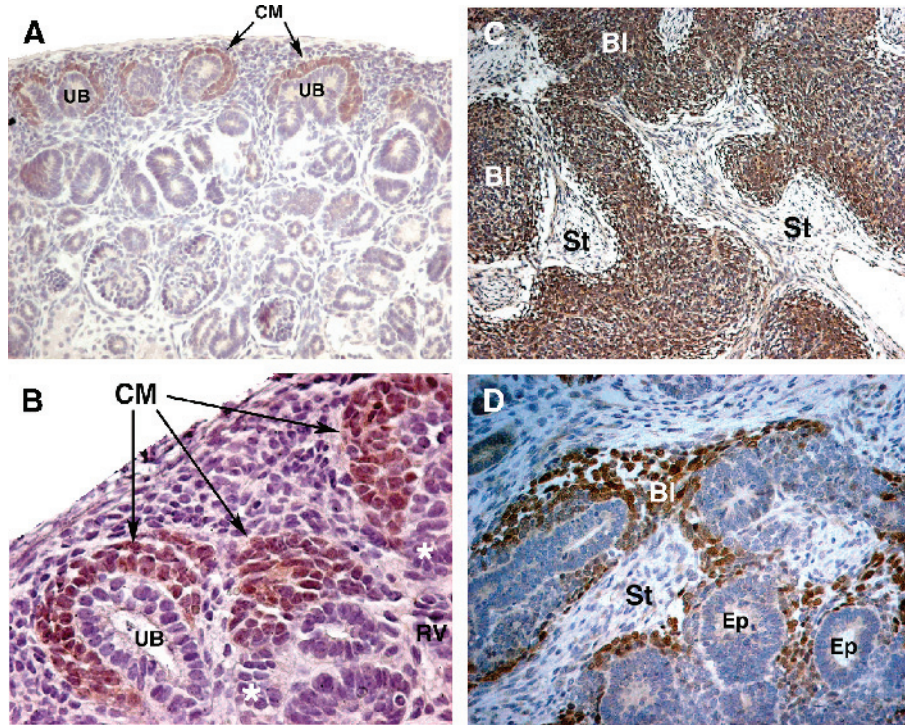


**Figure 3.** CITED1 immunoperoxidase staining of human fetal kidney (A and B) and Wilms' tumors (C and D). (A) Original magnification,  $\times 100$ ; (B) original magnification,  $\times 400$ . (A and B) As in the rat fetal kidney, CITED1 expression is restricted to the condensed metanephric mesenchyme (CM) immediately adjacent to and surrounding the UB. (B) The earliest epithelial structures of mesenchymal origin, pretubular aggregates (\*), and renal vesicles (RV) again show the absence of CITED1 expression in the human fetal kidney. (C) CITED1 expression is intense in malignant blastema (BI) but absent in stroma (St) (original magnification,  $\times 100$ ). (D) The region of blastemal-to-epithelial transition in human Wilms' tumor also shows a gradient of CITED1 expression from intense in peripheral blastema to absent in central epithelia (Ep) (original magnification,  $\times 400$ ).

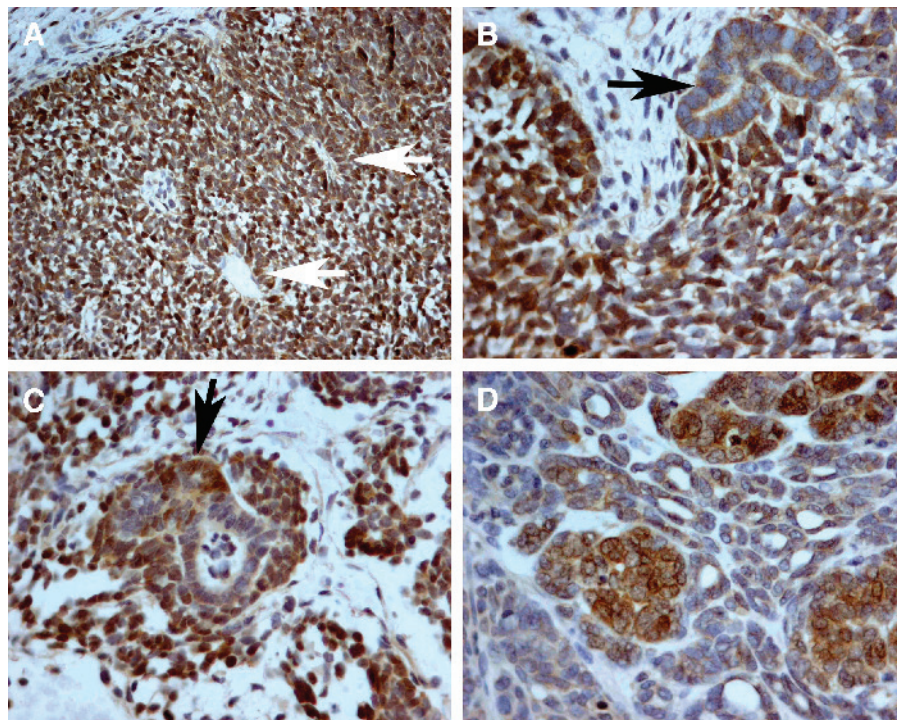


**Figure 4.** CITED1 expression was detected in certain primitive epithelial structures of human Wilms' tumors. (A) Primitive tubular structures in the form of rosettes show CITED1 expression (white arrows) (original magnification,  $\times 200$ ). (B) A more mature-appearing epithelial structure shows a weak cytoplasmic expression of CITED1 (black arrow) (original magnification,  $\times 400$ ). (C) CITED1 expression in certain tumor regions shows an intensity gradient from greater cytoplasmic expression in peripheral blastemal cells (also lacking organized architecture) to weak cytoplasmic expression in the more organized tubular portion (black arrow) (original magnification,  $\times 400$ ). (D) Primitive tubules and epithelial elements showing intermediate CITED1 expression (original magnification,  $\times 400$ ).

**Table 2.** Intensity and Subcellular Localization of CITED1 in Blastemal or Epithelial Elements, Arranged in Ascending Order of Disease Stage.

Stage	Optical Density of CITED1 Content	COG Pathology of Original Specimen	Blastema		Epithelia		Pathology of Specimen Received
			Nucleus	Cytoplasm	Nucleus	Cytoplasm	
I	73.9193	Mixed	Intermediate	Intermediate	Absent	Weak	Blastemal predominant
I	142.956	Mixed	Weak	Intermediate			
I	161.329	Mixed	Weak	Strong	Absent	Intermediate	
I	175.217	Mixed	Strong	Intermediate	Absent	Weak	Epithelial predominant
I	225.351	Epithelial undifferentiated			Strong	Intermediate	
II	97.6555	Mixed			Absent	Intermediate	
II	136.057	Mixed	Intermediate	Intermediate	Absent	Weak	Blastemal predominant
II	190.715	Blastemal	Intermediate	Strong			
II	197.219	Mixed	Intermediate	Intermediate	Absent	Weak	
III	93.3567	Mixed	Weak	Strong	Absent	Intermediate	Blastemal predominant
III	104.387	Mixed	Intermediate	Intermediate			
III	180.112	Mixed	Strong	Intermediate	Weak	Intermediate	
III	220.589	Mixed	Strong	Intermediate			Blastemal predominant
IV	223.771	Mixed	Weak	Strong	Weak	Intermediate	
IV	236.798	Mixed			Absent	Intermediate	
IV	241.154	Blastemal	Intermediate	Strong			Epithelial predominant
IV	241.407	Blastemal	Strong	Intermediate			
IV	300.985	Blastemal	Strong	Strong			
V	158.057	Mixed	Strong	Intermediate	Absent	Weak	Blastemal predominant
V	299.851	Mixed	Strong	Strong	Absent	Weak	

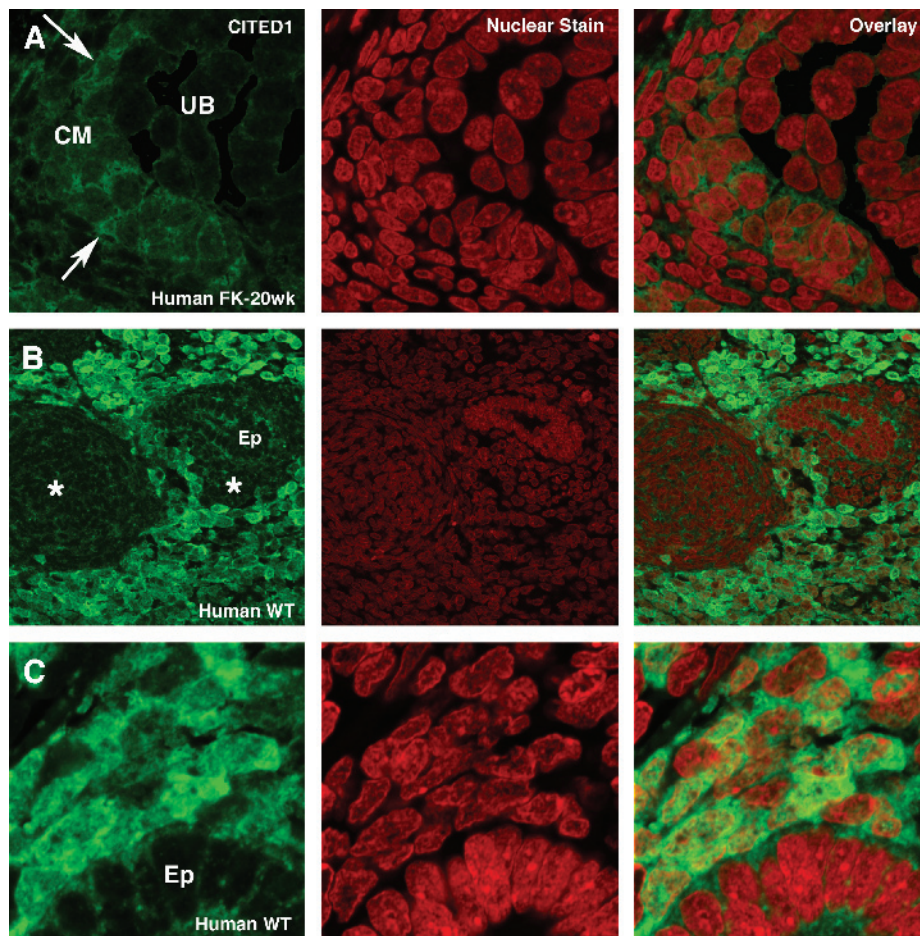


**Figure 5.** CITED1 immunofluorescent staining of human fetal kidney (FK; row A) and Wilms' tumor (WT; rows B and C). CITED1 and TO-PRO3 nuclear stain are represented in green and red, respectively. (Row A) CITED1 expression is restricted to the condensed metanephric mesenchyme (CM) and is localized predominantly in the cytoplasm (white arrows) (original magnification,  $\times 630$ ). (Rows B and C) CITED1 expression is intense in malignant blastema and, in contrast to the embryonic state, is robustly detected in the nuclei of this cell population. (B) Aggregating and differentiating blastema (\*) show downregulation of CITED1 expression relative to surrounding disorganized blastemas (bright green; Ep = epithelia) (original magnification,  $\times 400$ ). (C) High-power view of malignant blastema showing a rich nuclear accumulation of CITED1 (Ep = epithelia) (original magnification,  $\times 630$ ).

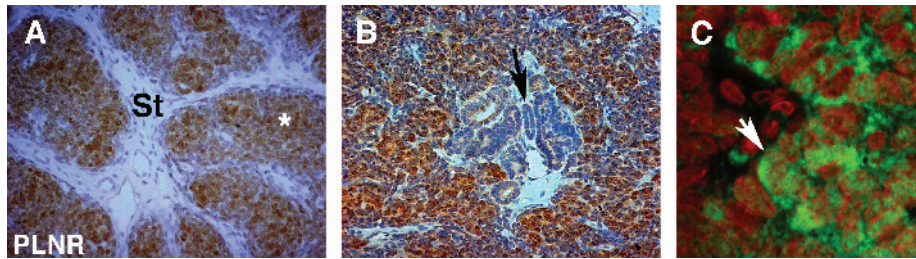


**Figure 6.** *CITED1* expression in human perilobar nephrogenic rests (PLNRs). (A) Immunoperoxidase staining shows that *CITED1* expression is rich in blastemal structures (\*) but absent in stroma (St) (original magnification,  $\times 200$ ). (B) Intensity gradient of *CITED1* expression from strong in peripheral undifferentiated blastema to reduced or absent in clearly defined tubular elements (black arrow) (original magnification,  $\times 200$ ). (C) Variable cytoplasmic and nuclear localizations of *CITED1* in blastemal elements (original magnification,  $\times 630$ ).

To confirm these immunohistochemical analyses, we also performed *in situ* hybridization to evaluate *CITED1* mRNA expression in experimental rat and human Wilms' tumors. As shown in Figure 7, high levels of *CITED1* mRNA were restricted to blastemal elements of both rat and human nephroblastomas. Analogous to protein expression studies, *CITED1* mRNA was not detected in epithelial or stromal elements of the tumors examined.

#### *CITED1* Content in Primary Human Wilms' Tumors and Stage of Disease

We compared *CITED1* expression in the 20 COG Wilms' tumor samples to determine whether its cellular distribution or subcellular localization varied among tumor stages I to V.

Wilms' tumor stage is a clinical variable based on tumor volume and spread, and it is not influenced by the histologic appearance of tumors [24]. In our studies, *CITED1* was widely expressed in all tumor stages, yet showed the strongest immunostaining within blastemal compartments of higher stage malignancies (stages III–V; Table 2). Furthermore, in localized disease stages I and II ( $n = 9$ ), *CITED1* showed strong nuclear expression in only two specimens, whereas in more advanced stages (stages III–V), nuclear expression of *CITED1* was characterized as strong in 6 of 11 tissue samples (Table 2).

To further evaluate these immunohistochemical observations, we quantified *CITED1* protein expression in all 20 COG Wilms' tumor samples by Western blot analysis. Despite the

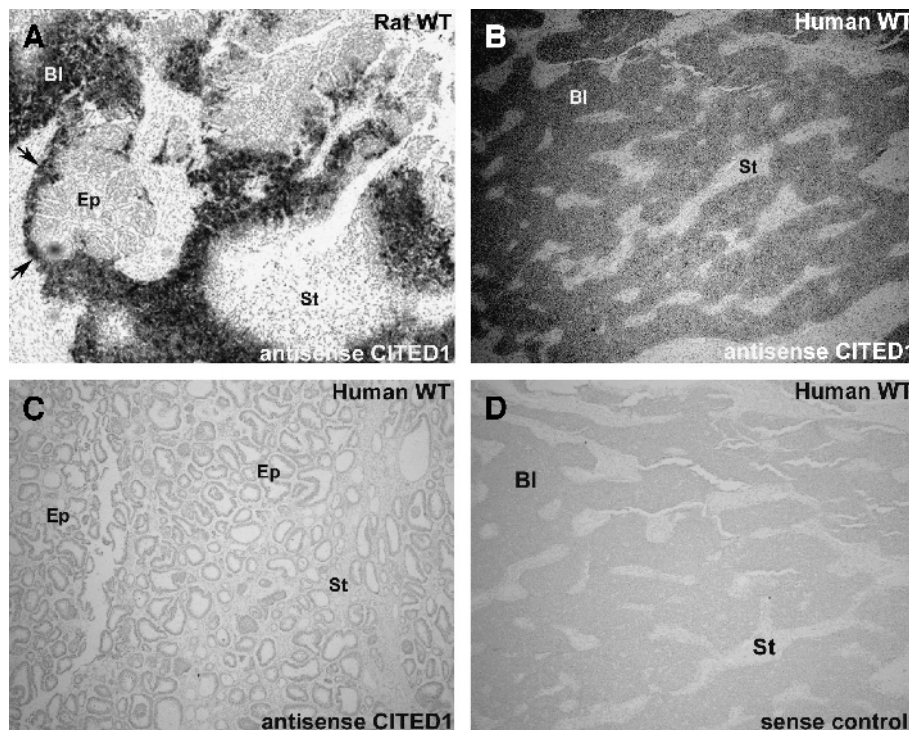


**Figure 7.** *In situ* hybridization detects *CITED1* mRNA in rat (A) and human (B–D) nephroblastoma (WT). (A) Rat WT shows that *CITED1* mRNA is restricted to blastemal compartments (Bl; dark regions). *CITED1* mRNA is also detected in peripheral blastema (arrows) immediately surrounding more differentiated tumor epithelia (Ep). Epithelial and stromal (St) compartments do not express *CITED1* mRNA. (B) Human WT shows *CITED1* mRNA restriction to blastemal compartments (Bl; dark regions) and absence in stroma (St). (C) Epithelial-predominant human WT showing no detection of *CITED1* mRNA in either epithelia (Ep) or stroma (St). (D) Sense control showing no detection of radiolabeled probe.



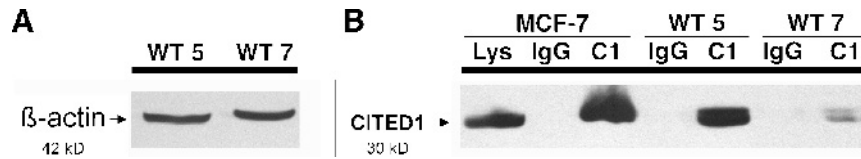


**Figure 8.** Representative Western blot analysis for CITED1 after immunoprecipitation (IP). (A)  $\beta$ -Actin control Western blot analysis of tissue lysates performed to confirm that equal quantities of sample protein were immunoprecipitated for CITED1. (B) CITED1 (C1) bands after initial immunoprecipitation using a rabbit anti-CITED1 antibody, and subsequent Western blot analysis (WB) using the mouse anti-CITED1 monoclonal antibody 2h6. CITED1 migrates as a doublet in several WT specimens. The MCF-7 breast carcinoma cell line served as a CITED1-positive control [18]. Rabbit IgG was used as a negative control for immunoprecipitation. WT-5 and WT-7 represent different Wilms' tumor samples expressing different quantities of CITED1.

strong blastemal immunostaining noted above, initial experiments performed to detect CITED1 expression in whole tumor lysates failed, presumably the result of diluting total protein from CITED1-expressing cells with other nonexpressing cellular elements within tumors (epithelia and stroma). We therefore enriched the CITED1 content of tumor lysates by immunoprecipitation using an anti-CITED1 antibody (Figure 8). As shown in Figure 8, several Wilms' tumor specimens express a CITED1 doublet that likely reflects protein phosphorylation—a posttranslational modification that we have demonstrated as occurring in proliferating cells [18].

Compared to patients presenting with disease at stages I to III, patients with metastatic stage IV disease ( $n = 5$ ) at diagnosis had significantly greater CITED1 protein content in primary tumors ( $P = .0033$ ; Figure 9A). The two specimens obtained from patients presenting with bilateral stage V disease also had a higher mean CITED1 protein content in primary tumors, but this difference did not reach statistical significance possibly because of low numbers assayed from this stage ( $P = .08$ ). Notably, we did not receive any further substaging criteria for these two stage V tumors. However, after adjusting for the differences in CITED1 protein content seen by disease stage, CITED1 content in primary Wilms' tumors was not different between patients who developed disease relapse and those who did not ( $P = .88$ ). A review of tumor sample histology did not associate the greater CITED1 protein content with blastemal predominance of stage IV tumors. This observation suggests that the increased expression of CITED1 in stage IV tumors does not simply result

from increased numbers of blastemal cells, but that CITED1 expression is upregulated in malignant blastema.

Exploratory data analysis showed further that the CITED1 protein content of primary Wilms' tumors appeared to associate with the gender and age of a child at presentation for patients with localized disease (stages I–III). After adjusting for differences in CITED1 protein content according to disease stage, the CITED1 content of primary tumors for females aged > 4 years ( $n = 4$ ) was greater than that for all other gender–age groups presenting with nonmetastatic disease (Figure 9B). Regression analysis showed that CITED1 values for females aged > 4 years were significantly greater ( $P = .003$ ) than those for females presenting at < 4 years ( $n = 4$ ) or for any aged male ( $n = 5$ ), and that these values approached those for patients presenting with metastatic disease.

## Discussion

In these studies, we have characterized for the first time the blastemal expression of the transcriptional regulator CITED1 in human and NEU-induced rat Wilms' tumors. Our findings demonstrate that CITED1 is consistently expressed in disorganized blastemal cells of both human and experimental Wilms' tumors and of the putative precursor lesions, perilobar nephrogenic rests. We show further that CITED1 is clearly detected in the nuclear compartment of transformed blastema relative to its predominantly cytoplasmic localization in embryonic metanephric mesenchyme. Interestingly, in both human and rat tumors, CITED1 is expressed most

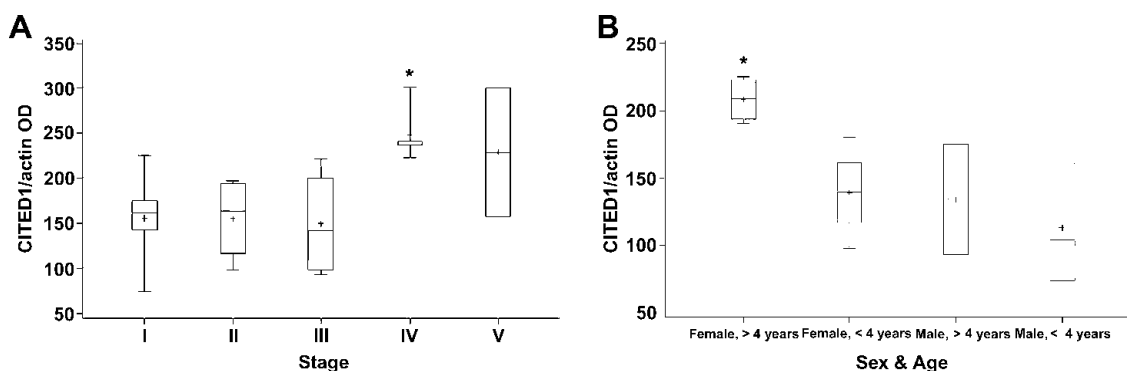


**Figure 9.** (A) The CITED1 protein content of primary Wilms' tumors, as estimated by the ratio of Western blot optical densities of specimen CITED1 to  $\beta$ -actin bands (vertical axis), was associated with advanced stage IV disease. The total number of patients per stage and the absolute values of CITED1 content per tumor are shown in Table 2. The CITED1 content of primary stage IV tumors was compared to that for stages I to III.  $*P = .0033$ . (B) CITED1 protein content was also highest in the primary Wilms' tumors of girls presenting beyond 4 years of age. The CITED1 content of primary WT arising in girls aged > 4 years ( $n = 4$ ) was compared to that arising in girls presenting at < 4 years ( $n = 4$ ) or to that arising in boys at any age ( $n = 5$ ).  $*P = .003$ .

intensely along the outer cells of undifferentiated blastema that surround aggregates of more differentiated elements. Finally, we have shown that the level of CITED1 expression in primary Wilms' tumors correlates with tumor stage. Taken together, these observations are consistent with the hypothesis that Wilms' tumor blastema are derived from the abnormal postnatal retention of the condensed metanephric mesenchyme within the adult kidney, and establish CITED1 as a new histologic marker of malignant blastema. Furthermore, the correlation of our human tumor findings with chemically induced rat nephroblastomas confirms that the latter is a good model of the human disease.

The highest expression levels of CITED1 were detected in primary Wilms' tumors of children presenting with advanced stage IV disease, implicating this transcriptional regulator as a marker of disease severity. Other cell-based and tumor-based markers, including telomerase [25], IGFR-I [26], topoisomerase II [27], and CRABP2 [28,29], have been associated with adverse Wilms' tumor behaviors; in a heterotransplant model of human Wilms' tumor, increasing serum hyaluronan concentrations have been associated with more aggressive Wilms' tumor biology [30]. None of these factors, however, has been clearly associated with the cellular function of embryonic condensed metanephric mesenchyme. Previous microarray studies have shown that a number of genes involved in nephrogenesis, yet normally downregulated in the adult kidney, are overrepresented in Wilms' tumor specimens. These metanephric mesenchyme genes include *WT1* [12], *PAX2* [13], *SIX1*, *EYA1*, *SALL2*, and *HOXA11* [10]. However, these studies do not establish the precise cellular distribution or regulation of gene expression, either within the tumors themselves or in different tumor stages. Using a highly specific and commercially available anti-CITED1 antibody, we have been able to map carefully the expression of this developmentally regulated protein in embryonal Wilms' tumors. Our observation that CITED1 shows a gradient of expression (highest in the outer cells of blastemal compartments that surround histologically more differentiated, CITED1-negative tumor elements) provides the first evidence that this population of undifferentiated cells may be undergoing progressive epithelial transition. This pattern of differentiation caricatures the normal induction of the condensed metanephric mesenchyme within the developing kidney and suggests that active inductive signaling modifies the cellular composition of Wilms' tumors. Unlike the developing kidney, however, CITED1 is detected in primitive tumor epithelia, suggesting further that these cells may represent an intermediate embryonic phenotype not normally seen in development. In contrast, the observation that CITED1 is never detected in stromal elements suggests that the ontogeny of this cell population is distinct from blastemal and epithelial elements in Wilms' tumors.

Altered subcellular localization of CITED1 in Wilms' tumors was an unexpected finding and suggests that its regulation could play a role in Wilms' tumor initiation and pathogenesis. Distinct from the dominant cytoplasmic localization of CITED1 in the condensed metanephric mesenchyme, CITED1 is equally distributed between the nuclear

compartment and the cytoplasmic compartment of Wilms' tumor blastema. This phenomenon is also seen in diffusely hyperplastic perilobar nephrogenic rests containing premalignant Wilms' tumor precursor cells, indicative that change in the subcellular localization of CITED1 occurs early in the course of the disease. We have previously shown that CITED1 contains a strong nuclear export signal within its C-terminal transactivation domain [18]. The mixed nuclear–cytoplasmic distribution of CITED1 in Wilms' tumors is consistent with loss of nuclear export signal function, but how this mechanism is perturbed in malignant cells remains unknown. Interestingly, the related family member CITED4 has been shown to shift from a predominantly nuclear localization to the cytoplasm during the transformation of normal tissue to malignant breast tissue [31], suggesting a possible conservation of mechanisms regulating subcellular localization in this family of proteins and contributing to neoplasia.

Our *in situ* hybridization data support the concept that CITED1 gene transcription is dysregulated in Wilms' tumor pathogenesis, yet its functional contributions to nephroblastoma initiation and progression remain unclear. High levels of CITED1 expression could simply be a marker of blastemal persistence in these tumors; however, our studies show that the level of CITED1 expression correlates with tumor stage independently of blastemal content in Wilms' tumors, suggesting a direct role for CITED1 in Wilms' tumor progression. Additionally, the observation that CITED1 is localized to the nucleus of blastema within the precursor lesions, nephrogenic rests, implicates a further role in Wilms' tumor initiation. There exist two alternative mechanisms, although not necessarily mutually exclusive, by which CITED1 could influence Wilms' tumorigenesis. First, high cellular levels of CITED1 could exert a direct oncogenic effect on blastemal cells. This explanation is supported by the observation that high levels of CITED1 have been associated not only with Wilms' tumors but also with malignancies of the thyroid gland [32], and skin [33]. Furthermore, we have shown that overexpression of CITED1 in the human Wilms' tumor cell line SK-NEP-1 enhances cellular proliferation *in vitro*, whereas overexpression of a truncated functionally inactive *CITED1* mutant perturbs this effect *in vitro* and tumorigenesis *in vivo* [22]. As SK-NEP-1 cells have not been shown to differentiate or to form epithelial structures in heterotransplant models, it is likely that overexpression of this dominant-negative *CITED1* mutant modifies SK-NEP-1 tumorigenesis by perturbing cellular proliferative capacity and survival more than inducing cellular differentiation.

A second possible mechanism is that persistent expression of CITED1 in metanephric blastema could play an adverse developmental role in the pathogenesis of these tumors. We have previously shown that overexpression of CITED1 in cultured embryonic kidneys interferes with organized differentiation of the condensed metanephric mesenchyme [17]. This observation suggests that dysregulated CITED1 expression could play a role in preventing the organized differentiation of the metanephric mesenchyme, thereby promoting the persistence of metanephric blastema in postnatal kidneys of Wilms' tumor patients. This hypoth-

esis is consistent with the observation that CITED1 overexpression inhibits Wnt/ $\beta$ -catenin–dependent transcriptional responses [17], as Wnt signaling promotes epithelial differentiation of the metanephric mesenchyme *in vivo* [34,35]. Indeed, activating mutations of  $\beta$ -catenin have been described in 10% to 15% of Wilms' tumors [36–38]. Subsequent evidence that an even higher percentage of sporadic Wilms' tumors shows stabilization and nuclear accumulation of  $\beta$ -catenin has emerged [39]. Furthermore, more recent studies have identified inactivating mutations in the X-linked gene *WTX* in 30% of Wilms' tumors [40], and *WTX* is an essential component of the  $\beta$ -catenin destruction complex [41]. These findings raise the possibility that increased levels of CITED1 expression in metanephric blastema could play a role in preventing Wnt-dependent epithelial differentiation in established Wilms' tumors.

Finally, the primary tumors of girls aged > 4 years showed the highest CITED1 protein content, which is of interest because the gene locus for CITED1 is found on the X chromosome [42]. Furthermore, CITED1 has been shown to function as a selective coactivator of estrogen-dependent transcription [43]. In a recent Danish population-based study, investigators showed that the risk of developing Wilms' tumor increased with excessive fetal growth in girls and decreased with fetal growth in boys, although the findings did not reach statistical significance [44]. Nevertheless, we do not know the serum estrogen content of the patients in our study, nor do we understand the functional significance of CITED1 and estrogen interactions in Wilms' tumor pathogenesis. The influence of maternal estrogen on the persistence of embryonic blastemal elements remains only speculative.

In summary, we have characterized the expression patterns of CITED1 in two models of nephroblastoma. We have shown that CITED1, which is normally expressed in the condensed metanephric mesenchyme and downregulated in the postnatal kidney, persists as a marker of blastema cells in both premalignant nephrogenic rests and malignant Wilms' tumors. Furthermore, our studies show that CITED1 localizes to the nucleus of Wilms' tumor blastema and that the level of CITED1 expression in the transformed blastema of primary human Wilms' tumors correlates with the stage of the disease. These findings indicate that CITED1 is a novel marker of Wilms' tumor blastema and suggest that persistent expression and/or altered subcellular localization of CITED1 could play a role in the initiation and pathogenesis of Wilms' tumors.

### Acknowledgements

The authors thank Toshi Shioda for graciously providing the anti-CITED1 antibody 2h6. We also are indebted to Jeffrey Dome and the COG for providing human Wilms' tumor specimens and insightful assistance with this study.

### References

- [1] Saxen L and Sariola H (1987). Early organogenesis of the kidney. *Pediatr Nephrol* **1**, 385–392.
- [2] Dressler GR (2006). The cellular basis of kidney development. *Annu Rev Cell Dev Biol* **22**, 509–529.
- [3] Beckwith JB (1997). New developments in the pathology of Wilms tumor. *Cancer Invest* **15**, 153–162.
- [4] Schmidt D and Beckwith JB (1995). Histopathology of childhood renal tumors. *Hematol/Oncol Clin North Am* **9**, 1179–1200.
- [5] Beckwith JB, Kiviat NB, and Bonadio JF (1990). Nephrogenic rests, nephroblastomatosis, and the pathogenesis of Wilms' tumor. *Pediatr Pathol* **10**, 1–36.
- [6] Haber DA, Buckler AJ, Glaser T, Call KM, Pelletier J, Sohn RL, Douglass EC, and Housman DE (1990). An internal deletion within an 11p13 zinc finger gene contributes to the development of Wilms' tumor. *Cell* **61**, 1257–1269.
- [7] Bruening W, Bardeesy N, Silverman BL, Cohn RA, Machin GA, Aronson AJ, Housman D, and Pelletier J (1992). Germline intronic and exonic mutations in the Wilms' tumour gene (*WT1*) affecting urogenital development. *Nat Genet* **1**, 144–148.
- [8] Kreidberg JA, Sariola H, Loring JM, Maeda M, Pelletier J, Housman D, and Jaenisch R (1993). WT-1 is required for early kidney development. *Cell* **74**, 679–691.
- [9] Li W, Kessler P, and Williams BR (2005). Transcript profiling of Wilms tumors reveals connections to kidney morphogenesis and expression patterns associated with anaplasia. *Oncogene* **24**, 457–468.
- [10] Li CM, Guo M, Borczuk A, Powell CA, Wei M, Thaker HM, Friedman R, Klein U, and Tycko B (2002). Gene expression in Wilms' tumor mimics the earliest committed stage in the metanephric mesenchymal–epithelial transition. *Am J Pathol* **160**, 2181–2190.
- [11] Dekel B, Metsuyanin S, Schmidt-Ott KM, Fridman E, Jacob-Hirsch J, Simon A, Pinthus J, Mor Y, Barasch J, Amariglio N, et al. (2006). Multiple imprinted and stemness genes provide a link between normal and tumor progenitor cells of the developing human kidney. *Cancer Res* **66**, 6040–6049.
- [12] Grubb GR, Yun K, Williams BR, Eccles MR, and Reeve AE (1994). Expression of WT1 protein in fetal kidneys and Wilms tumors. *Lab Invest* **71**, 472–479.
- [13] Dressler GR and Douglass EC (1992). Pax-2 is a DNA-binding protein expressed in embryonic kidney and Wilms tumor. *Proc Natl Acad Sci USA* **89**, 1179–1183.
- [14] Sharma PM, Bowman M, Yu BF, and Sukumar S (1994). A rodent model for Wilms tumors: embryonal kidney neoplasms induced by *N*-nitroso-*N'*-methylurea. *Proc Natl Acad Sci USA* **91**, 9931–9935.
- [15] Hard GC (1985). Differential renal tumor response to *N*-ethylnitrosourea and dimethylnitrosamine in the Nb rat: basis for a new rodent model of nephroblastoma. *Carcinogenesis* **6**, 1551–1558.
- [16] Higinbotham KG, Karavanova ID, Diwan BA, and Perantoni AO (1998). Deficient expression of mRNA for the putative inductive factor bone morphogenetic protein-7 in chemically initiated rat nephroblastomas. *Mol Carcinog* **23**, 53–61.
- [17] Plisov S, Tsang M, Shi G, Boyle S, Yoshino K, Dunwoodie SL, Dawid IB, Shioda T, Perantoni AO, and de Caestecker MP (2005). Cited1 is a bifunctional transcriptional cofactor that regulates early nephronic patterning. *J Am Soc Nephrol* **16**, 1632–1644.
- [18] Shi G, Boyle SC, Sparrow DB, Dunwoodie SL, Shioda T, and de Caestecker MP (2006). The transcriptional activity of CITED1 is regulated by phosphorylation in a cell cycle–dependent manner. *J Biol Chem* **281**, 27426–27435.
- [19] Boyle SC, Shioda T, Perantoni AO, and de Caestecker MP (2007). Cited1 and Cited2 are differentially expressed in the developing kidney but are not required for nephrogenesis. *Dev Dyn* [Epub July 5].
- [20] Green DM (1997). Wilms' tumour. *Eur J Cancer* **33**, 409–418, discussion, 419–420.
- [21] Perantoni AO, Timofeeva O, Naillat F, Richman C, Pajni-Underwood S, Wilson C, Vainio S, Dove LF, and Lewandoski M (2005). Inactivation of FGF8 in early mesoderm reveals an essential role in kidney development. *Development* **132**, 3859–3871.
- [22] Lovvorn HN III, Boyle S, Shi G, Shyr Y, Wills ML, Perantoni AO, and de Caestecker M (2007). Wilms' tumorigenesis is altered by misexpression of the transcriptional co-activator, CITED1. *J Pediatr Surg* **42**, 474–481.
- [23] Shioda T, Fenner MH, and Isselbacher KJ (1996). *msg1*, a novel melanocyte-specific gene, encodes a nuclear protein and is associated with pigmentation. *Proc Natl Acad Sci USA* **93**, 12298–12303.
- [24] Green DM (2004). The treatment of stages I–IV favorable histology Wilms' tumor. *J Clin Oncol* **22**, 1366–1372.
- [25] Dome JS, Bockhold CA, Li SM, Baker SD, Green DM, Perlman EJ, Hill DA, and Breslow NE (2005). High telomerase RNA expression level is an adverse prognostic factor for favorable-histology Wilms' tumor. *J Clin Oncol* **23**, 9138–9145.
- [26] Natrajan R, Reis-Filho JS, Little SE, Messahel B, Brundler MA, Dome JS, Grundy PE, Vujanec GM, Pritchard-Jones K, and Jones C (2006).

- Blastemal expression of type I insulin-like growth factor receptor in Wilms' tumors is driven by increased copy number and correlates with relapse. *Cancer Res* **66**, 11148–11155.
- [27] Tretiakova M, Turkyilmaz M, Grushko T, Kocherginsky M, Rubin C, Teh B, and Yang XJ (2006). Topoisomerase IIalpha in Wilms' tumour: gene alterations and immunoeexpression. *J Clin Pathol* **59**, 1272–1277.
- [28] Natrajan R, Williams RD, Hing SN, Mackay A, Reis-Filho JS, Fenwick K, Irvani M, Valgeirsson H, Grigoriadis A, Langford CF, et al. (2006). Array CGH profiling of favourable histology Wilms tumours reveals novel gains and losses associated with relapse. *J Pathol* **210**, 49–58.
- [29] Takahashi M, Yang XJ, Lavery TT, Furge KA, Williams BO, Tretiakova M, Montag A, Vogelzang NJ, Re GG, Garvin AJ, et al. (2002). Gene expression profiling of favorable histology Wilms tumors and its correlation with clinical features. *Cancer Res* **62**, 6598–6605.
- [30] Lovvorn HN III, Savani RC, Ruchelli E, Cass DL, and Adzick NS (2000). Serum hyaluronan and its association with unfavorable histology and aggressiveness of heterotransplanted Wilms' tumor. *J Pediatr Surg* **35**, 1070–1078.
- [31] Fox SB, Braganca J, Turley H, Campo L, Han C, Gatter KC, Bhattacharya S, and Harris AL (2004). CITED4 inhibits hypoxia-activated transcription in cancer cells, and its cytoplasmic location in breast cancer is associated with elevated expression of tumor cell hypoxia-inducible factor 1alpha. *Cancer Res* **64**, 6075–6081.
- [32] Prasad ML, Pellegata NS, Kloos RT, Barbacioru C, Huang Y, and de la Chapelle A (2004). CITED1 protein expression suggests papillary thyroid carcinoma in high throughput tissue microarray-based study. *Thyroid* **14**, 169–175.
- [33] Li H, Ahmed NU, Fenner MH, Ueda M, Isselbacher KJ, and Shioda T (1998). Regulation of expression of MSG1 melanocyte-specific nuclear protein in human melanocytes and melanoma cells. *Exp Cell Res* **242**, 478–486.
- [34] Carroll TJ, Park JS, Hayashi S, Majumdar A, and McMahon AP (2005). Wnt9b plays a central role in the regulation of mesenchymal to epithelial transitions underlying organogenesis of the mammalian urogenital system. *Dev Cell* **9**, 283–292.
- [35] Kispert A, Vainio S, and McMahon AP (1998). Wnt-4 is a mesenchymal signal for epithelial transformation of metanephric mesenchyme in the developing kidney. *Development* **125**, 4225–4234.
- [36] Koesters R, Ridder R, Kopp-Schneider A, Betts D, Adams V, Niggli F, Briner J, and von Knebel Doeberitz M (1999). Mutational activation of the *beta-catenin* proto-oncogene is a common event in the development of Wilms' tumors. *Cancer Res* **59**, 3880–3882.
- [37] Maiti S, Alam R, Amos CI, and Huff V (2000). Frequent association of beta-catenin and *WT1* mutations in Wilms tumors. *Cancer Res* **60**, 6288–6292.
- [38] Li CM, Kim CE, Margolin AA, Guo M, Zhu J, Mason JM, Hensle TW, Murty VV, Grundy PE, Fearon ER, et al. (2004). *CTNNB1* mutations and overexpression of Wnt/beta-catenin target genes in *WT1*-mutant Wilms' tumors. *Am J Pathol* **165**, 1943–1953.
- [39] Koesters R, Niggli F, von Knebel Doeberitz M, and Stallmach T (2003). Nuclear accumulation of beta-catenin protein in Wilms' tumours. *J Pathol* **199**, 68–76.
- [40] Rivera MN, Kim WJ, Wells J, Driscoll DR, Brannigan BW, Han M, Kim JC, Feinberg AP, Gerald WL, Vargas SO, et al. (2007). An X chromosome gene, *WTX*, is commonly inactivated in Wilms tumor. *Science* **315**, 642–645.
- [41] Major MB, Camp ND, Berndt JD, Yi X, Goldenberg SJ, Hubbert C, Biechele TL, Gingras AC, Zheng N, Maccoss MJ, et al. (2007). Wilms tumor suppressor *WTX* negatively regulates WNT/beta-catenin signaling. *Science* **316**, 1043–1046.
- [42] Fenner MH, Parrish JE, Boyd Y, Reed V, MacDonald M, Nelson DL, Isselbacher KJ, and Shioda T (1998). *MSG1* (melanocyte-specific gene 1): mapping to chromosome Xq13.1, genomic organization, and promoter analysis. *Genomics* **51**, 401–407.
- [43] Yahata T, Shao W, Endoh H, Hur J, Coser KR, Sun H, Ueda Y, Kato S, Isselbacher KJ, Brown M, et al. (2001). Selective coactivation of estrogen-dependent transcription by CITED1 CBP/p300-binding protein. *Genes Dev* **15**, 2598–2612.
- [44] Jepsen P, Olsen ML, Mellemkjaer L, Olsen JH, and Sorensen HT (2004). A registry-based study of gender, fetal growth, and risk of Wilms tumor. *Pediatr Hematol Oncol* **21**, 435–439.